[Article ID] 1003- 6326(2001)04- 0551- 04

Intercalation mechanisms of lithium into graphitized needle cokes①

SU Yu-chang(苏玉长)[1], YING Zhi-min(尹志民)[1], XU Zhong-yu(徐仲榆)[2]
(1. Department of Materials Science and Engineering, Central South University, Changsha 410083, P. R. China;
2. Institute of New carbon materials, Hunan University, Changsha 410082, P. R. China

[Abstract] A needle coke was graphitized at different heat treatment temperature (2 000 ℃ to 3 000 ℃). The electrochemical intercalation mechanism of Li into the graphitized coke has been studied in Lil 1 mol·$L^{-1}LiClO_4$+ ethylene carbonate/ diethylene carbonatel graphite cells, using an in-situ X-Ray diffraction (XRD) technique. The study of Li-C intercalation processes of the graphitized coke reveals that there are three major types of intercalation behavior. The first is uniformly intercalated at all Li-C compounds in graphitized coke heated at 2 250 ℃; the second is obviously staging phenomenon during intercalation for the graphitized coke heated at 2 750 ℃; the third is cointercalation of solvated Li-ion at high potential (> 0.3V) and then lithium electrochemical intercalation at lower potential for that heated at 3 000 ℃, resulting in the decrease of capacity and efficiency of graphite negative electrode for lithium-ion secondary battery.

[Key words] needle coke; graphitized; intercalation
[CLC number] TM 242 [Document code] A

1 INTRODUCTION

The knowledge about the mechanism of intercalation reaction of Li into graphite seems to be very lacking, compared to the fact that a number of carbon materials have been synthesized. In general, the amount of lithium intercalated and the chemical potential of intercalation depend on the structure of carbon. Petroleum coke is the most important raw material for the manufacture of artificial carbon and graphite, after high temperature heat treatment, the petroleum coke becomes good active substances for the negative electrode of lithium-ion rechargeable batteries[1~3]. The more graphitic the carbon, the higher its capacity and the more sensitive to the solution composition it is[4~10], thus graphite electrodes have a very limited cycle life in many solvent systems due to the destruction of graphitic structure (exfoliation)[5]. Therefore the most appropriate heat-treatment temperature (HTT_{max}) and degree of graphitization for the carbon material must be considered, otherwise the charging-discharging performance of the batteries will become poor. In this paper the results of the electrochemical intercalation of graphitized coke/lithium cells are presented, using in-situ X-ray diffraction analysis.

2 EXPERIMENTAL

A needle coke (ANC) was heated in a middle frequency oven at different HTT_{max}: 2000, 2250, 2500, 2750, and 3000 ℃. The graphitized products were ground <75 μm powders and were analyzed by X-ray diffraction with a SIEMEMS D5000 diffractometer equipped with a Co target X-ray tube and a diffracted-beam monochromator. From the width of the Bragg peaks, the average grain size was roughly calculated using the Scherrer equation.

$$L_{HKL}=\frac{\lambda}{\beta\cdot\cos\theta}$$

The powders were mixed with 10% polytetrafluoroethylene (PTFE) and were rolled by a heating roller to carbon membranes. After drying at 160 ℃ under vacuum, the carbon membranes were used as the electrodes of the lithium-ion rechargeable batteries to determine the galvanostatic charging-discharging capacity. The counter electrode and the reference electrode were made of metallic lithium foil, and the electrolyte was 1 mol/L $LiClO_4$ + ethylene carbonate (EC)/diethylene carbonate (DEC) (1∶1). During the galvanostatic charging-discharging, some samples were analyzed by in-situ X-ray diffraction simultaneously, which allowed us to monitor the changes of the graphitic structure at various depths of discharge and charge.

3 RESULTS AND DISCUSSION

The electrochemical characteristics of carbonaceous materials strongly depend on their morphology, crystallinity and orientation of crystallites, etc. In order to understand systematically the relationship between electrochemical properties of carbonaceous materials and its microstructure, it is convenient to investigate the effects of the maximum heat-treatment

① [Foundation item] Project (2000) supported by Foundation for University Key Teacher by the Ministry of Education
[Received date] 2001-03-31; [Accepted date] 2001-06-07

temperature.

The crystallite parameters d_{002} and L_c, L_{100} and L_{101} of the graphitized needle coke powders are shown in Table 1. From it we can see that d_{002} monotonously decrease with increasing HTT_{max} and L_{HKL} always increase with increasing HTT_{max}. The crystallite dimension in a-axis direction, L_{100}, increases very quickly. Therefore, for ANC300, it is difficult to examine the peak (100) and (101) by general $\theta \sim 2\theta$ couple scan, and the XRD pattern shows that ANC300 is a highly plane oriented material.

Table 1 Crystallite parameters of samples

Sample	HTT_{max} /℃	d_{002} /nm	L_{002} /nm	L_{100} /nm	L_{101} /nm
ANC200	2000	0.3419	21.2	20.4	2.1
ANC225	2250	0.3396	30.9	34.8	4.4
ANC250	2500	0.3369	42.6	52.8	6.5
ANC275	2750	0.3362	56.8	111.0	8.9
ANC300	3000	0.3355	71.4		

Three parameters are of particular importance in determining the quality of the graphite electrode. The first parameter is the reversible capacity that defines the capacity available from the electrode after the initial formation cycles, and it can be represented by the third discharging capacity. The second parameter is charging-discharging efficiency in the first cycle. The third parameter is the potential distribution.

The charging-discharging performance of the graphitized needle cokes used as the negative electrode is shown in Fig. 1. From it we can see that the discharging capacity (D_3) in the third cycle and charging-discharging efficiency (η_1) in the first cycle of graphitized needle cokes increase with increasing HTT_{max} below HTT_{max} = 2750 ℃, but decrease rapidly about 3000 ℃.

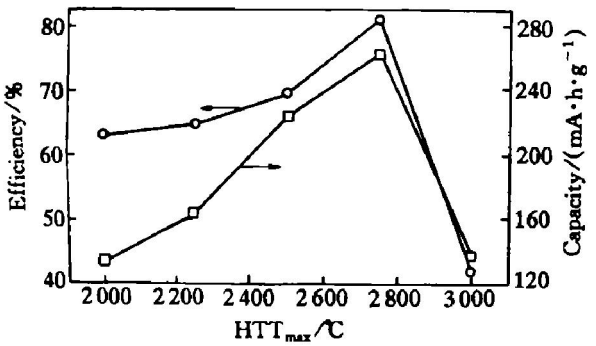

Fig. 1 Charging-discharging performance of graphitized needle cokes

Fig. 2 illustrates experimental potential-capacity curves for the first charge (intercalation) of Li/graphitized cokes cells. The entire charge encompasses three potential regions: a plateau region Ⅰ, a sloping region Ⅱ and a plateau region Ⅲ. A close examination reveals that the shape of the potential curves of potential regions are different with the increase of HTT_{max}. Plateau region Ⅰ becomes broader, the sloping region Ⅱ drops at high rates, and the plateau region Ⅲ become longer. The charge capacities in region Ⅱ (except ANC300) and in region Ⅲ are reversible, but it is irreversible in region Ⅰ.

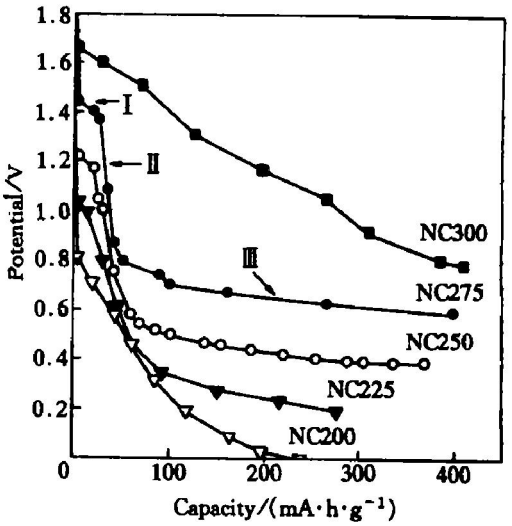

Fig. 2 Potential vs capacity for first charge of graphitized coke samples

The above results show that the charging-discharging performance of the graphitized needle cokes used as negative electrodes is related to their microstructure. Using in-situ X-ray diffraction, we examined the structure changes taking place in different samples during intercalation. The experiments reported here were done while Li was inserted into the graphitized samples; similar results were obtained during deintercalation.

Fig. 3 shows portions of in-situ X-ray profiles in the region of the graphite (002) peak taken from intercalation processes of sample ANC225. The potentials (vs Li/Li^+) at which XRD patterns were measured are indicated on Fig. 3. This peaks shift smoothly to lower angle as the cell potential decreases (as Li intercalates within the graphite). This shift corresponds to an increase of the (002) plane spacing due to the presence of Li between the layers. This evidence shows that Li is intercalated uniformly within the host material. However, the peak width at half maximum (FWHM) intensity of the corresponding peaks varies with potential. This broader peaks obtained reflects that different parts of the electrodes are at different stages at the same applied potential and illustrates that different parts of the sample are at different degree of graphitization in the same sample, resulting in lower discharging capacity.

Fig. 4 is the portions of in-situ X-ray diffraction spectra of sample ANC275 during intercalation pro-

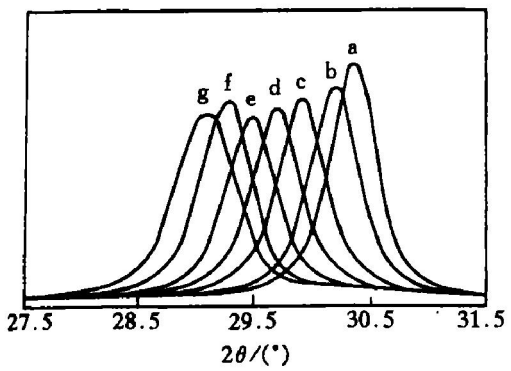

Fig.3 XRD spectra for (002) region of Li-GIC of sample ANC225

From a to g, scans were measured at following cell potentials: 1.50, 0.68, 0.42, 0.26, 0.12, 0 V, respectively

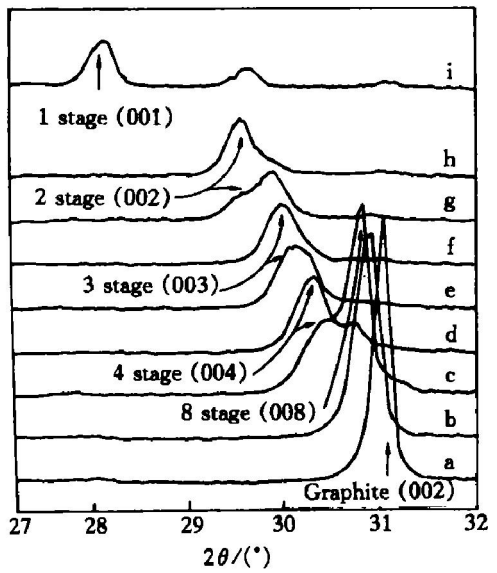

Fig.4 XRD spectra for (002) region of Li-GIC of sample ANC275

From a to i, scans were measured at following cell potentials: 1.50, 0.31, 0.20, 0.15, 0.12, 0.09, 0.06, 0.03, 0 V, respectively

cesses. From it we can see that the graphite intercalation process can be described by the stage index "n", which is equal to the number of graphite layers between two guest layers. The characteristic peaks of n stage and the potentials (vs Li/Li^+) at which XRD patterns were measured are indicated on Fig.4. From the XRD data collected at several degrees of intercalation the average interlayer distance d_n for nth-stage compound can be calculated according to that[9]:

$$d_n = d_i + n \times C_0 \quad (1)$$

where d_i is the thickness of one intercalation layer (such as LiC_6, $d_1 = 0.370$ nm, $d_i = 0.035$ nm) and C_0 means interlayer distance of graphite (0.336 nm). As a result, there are 1, 2, 3, 4 and 8 stage, and the experimental data show fairly good agreement with the calculated values. Coexistence of two-phases is observed by XRD in the eighth/fourth (Fig.4c and d), fourth/third (Fig.4 e), third/second (Fig.4 g) and second/first stages (Fig.4 i). Therefore, the Li-graphite intercalation processes of sample ANC275 are considered to undergo transitions of each stage according to eighth-stage—fourth-stage—third-stage—second-stage—first-stage. Since the theoretical capacity of 1 stage Li-GIC (LiC_6) is 372 mA·h/g, the sample ANC275 exhibits a larger capacity.

In order to learn why the cells with ANC300 reported in Fig.1 show poor discharging capacity and charging-discharging efficiency, an in-situ XRD experiment during charging-discharging processes was conducted. Fig.1 shows the potential-capacity curve, and Fig.5 shows the corresponding X-ray patterns. For the obtained XRD patterns, they show clearly different from the patterns in Fig.3 and Fig.4. As the charge process continues, the graphitic peaks become weaker and a new phase appears. This phase has two broad peaks nearby the (002) region of graphite, the leftward one centers at $2\theta \approx 28.0°$ (label I in Fig.5 scan c) and the other is of the rightward at $2\theta \approx 32.5°$ (label II in Fig.5 scan c). The leftward peak shifts smoothly to lower angle as the cell potential (>0.3 V) decreases and the rightward peak shifts to higher angle simultaneously. The appearance of peak II is a clear indication of staging that is the presence of intercalation of solvated Li-ion $Li(EC/DEC)^+$. To verify that the reaction mechanism for the ANC300 electrode is cointercalation of solvated Li-ion at higher potential (>0.3 V), the thickness of intercalated ion layer was calculated.

For scan c in Fig.5, the former peak I is iden-

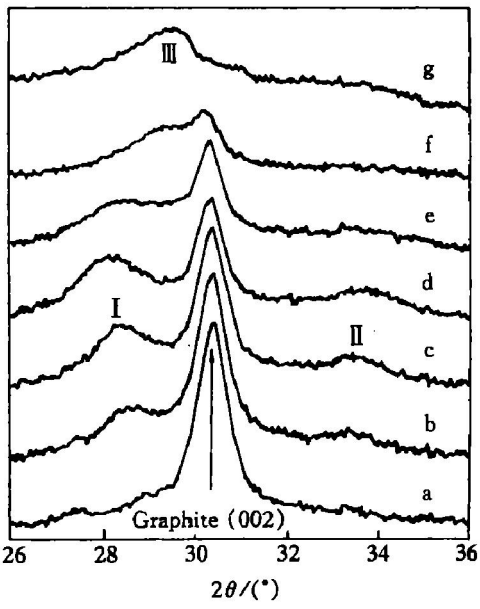

Fig.5 XRD spectra for (002) region of GIC of sample ANC300

From a to g, the scans were measured at following cell potential: 1.40, 0.82, 0.61, 0.41, 0.28, 0.13, 0V, respectively

tified as the $(00l)_n$ peak of a stage n structure, and the latter peak Ⅱ as the $(00l+1)_n$ peak. The peak index l can be calculated by

$$d_n = d_{\mathrm{I}} \times l = d_{\mathrm{II}} \times (l+1) \quad (2)$$

where d_n is the average interlayer distance for nth-stage compound, $d_{\mathrm{I}} = 0.370$ nm is the plane spacing of the $(00l)_n$ plane, and $d_{\mathrm{II}} = 0.317$ nm is the plane spacing of the $(00l+1)_n$ plane. Eqn. (2) is used to solve for l, and we can obtain

$$l = \frac{d_{\mathrm{II}}}{d_{\mathrm{I}} - d_{\mathrm{II}}} = 6$$

the d_n is calculated as

$$d_n = 0.370 \times l = 0.370 \times 6 = 2.22 \text{ (nm)}$$

From Eqn. (1) d_i is calculated as

$d_i(\min) = 2.22 - 6 \times 0.3355 = 0.207$ (nm), as $n_{\max} = 6$

and

$d_i = 2.22 - 5 \times 0.3355 = 0.543$ (nm), as $n = 5$, ($n = l - m_i$, $m_i = 0, 1, 2, \cdots, l-1$).

According to the situations of peak Ⅰ and peak Ⅱ, n should be 5, and the thickness of the intercalated ion layer is 0.543 nm.

Further charging leads to lithium ion intercalation in graphite and $Li(EC/DEC)^+$-GIC. The peaks I and II of $Li(EC/DEC)^+$-GIC become smaller and a new peak Ⅲ (center at $2\theta \approx 29.5°$) of Li-GIC appears.

Some works[5,6] were carried out on the intercalation process in several systems, resulting in different kinetic interpretations. The intercalation reaction in such a particular case as in lithium-ion secondary batteries may be divided into four elemental processes as follow:

1) adsorption of the intercalatent onto the surface of the host; 2) insertion of the intercalatent into the gallery of the host; 3) diffusion of the intercalatent in the gallery; 4) stage transition between different stage structures.

These results shown that the degree of graphitization, the L_{002}, L_{100} can not be too high to avoid the cointercalation of solvated Li-ion in graphitic microcrystallites at higher potential during charging.

4 CONCLUSION

There are three major types of intercalation behavior of Li into graphitized needle coke in 1 mol/L $LiClO_4$ + EC/DEC (1 : 1). In order to improve the charging-discharging performance of products, the appropriate maximum heat-treatment temperature must be considered. The HTT_{max} and the degree of graphitization have optimum values.

[REFERENCES]

[1] Guyomard D, Tarascaon J M. Li metal-free rechargeable $LiMn_2O_4$/carbon cells: their understanding and optimization [J]. J Electrochem Soc, 1992, 139(4): 937 - 948.

[2] Dahn J R, Sleigh A K, Shi H, et al. Dependence of the electrochemical intercalation of Lithium in carbons on the crystal structure of the carbon [J]. Electrochemica Acta, 1993, 38(9): 1179 - 1191.

[3] Endo M, Kim C, Nishimura K, et al. Recent development of carbon materials for Li ion batteries [J]. Carbon, 2000, 38: 183 - 197.

[4] Jiang W, Tran T, Song X, et al. Thermal and electrochemical studies of carbons for Li-ion batteries [J]. J Power Sources, 2000, 85: 261 - 178.

[5] Aurbach D, Ein-Eli Y. The study of Li-graphite intercalation processes in several electrolyte systems using in situ X-ray diffraction [J]. J Electrochem Soc, 1995, 142 (6): 1746 - 1752.

[6] Fujimoto H, Mabuchi A, Tokumitsu K, et al. Relationship between the charge capacity of a turbostratic carbon anode for a Li secondary battery and its structure [J]. Carbon, 2000, 38: 871 - 875.

[7] Guerin K, Fervier-Bouvier A, Flandrois S, et al. Effect of graphite crystal structure on lithium electrochemical intercalation [J]. J Electrochem Soc, 1999, 146(10): 3660 - 3665.

[8] Yamaki Jun-ichi, Egashira M, Okada S. Potential and thermodynamics of graphite anodes in Li-ion cells [J]. J Electrochem Soc, 2000, 147(2): 460 - 465.

[9] Dresselhaus M S, Dresselhaus G. Intercalation compounds of graphite [J]. Advances in Physics, 1981, 30 (2): 139 - 326.

[10] Dahn J R, Fong R, Spoon M J. Suppression of staging in lithium-intercalated carbon by disorder in the host [J]. Physical Review B, 1990, 42(10): 6424 - 6432.

(Edited by WU Jian-quan)